



POLİTEKNİK DERGİSİ

JOURNAL of POLYTECHNIC

ISSN: 1302-0900 (PRINT), ISSN: 2147-9429 (ONLINE)

URL: <http://dergipark.gov.tr/politeknik>



Li-ion battery thermal parameter identification and core temperature estimation

Li-ion pil termal parametre tanımlama ve çekirdek sıcaklık tahmini

Yazar(lar) (Author(s)): Khadija SAQLI¹, Houda BOUCHARÉB², Mohammed OUDGHIRI³, Kouider Nacer M'SIRDI⁴

ORCID¹: 0000-0003-2920-0359

ORCID²: 0000-0001-9548-9870

ORCID³: 0000-0002-9641-0770

ORICD⁴: 0000-0002-9485-6429

To cite to this article: Saqli K., Bouchareb H., Oudghiri M., M'SIRDI K. N., "Li-ion battery thermal parameter identification and core temperature estimation", *Journal of Polytechnic*, 26(4): 1495-1504, (2023).

Bu makaleye şu şekilde atıfta bulunabilirsiniz : Saqli K., Bouchareb H., Oudghiri M., M'SIRDI K. N., "Li-ion battery thermal parameter identification and core temperature estimation", *Politeknik Dergisi*, 26(4): 1495-1504, (2023).

Erişim linki (To link to this article): <http://dergipark.gov.tr/politeknik/archive>

DOI: 10.2339/politeknik.1161986

Li-Ion Battery Thermal Parameter Identification and Core Temperature Estimation

Highlights

- ❖ CFD simulation of the SOC and core temperature of the 18650 cylindrical LMO battery.
- ❖ Thermal parameter identification and validation of the two-state thermal battery model using the recursive least squares (RLS) method.
- ❖ Estimation of the battery core temperature using the Kalman filter (KF) approach.

Graphical Abstract

This study provides a comprehensive platform that uses CFD simulation to model and validate the battery thermal characteristics for accurately monitoring the battery core temperature using the KF method.

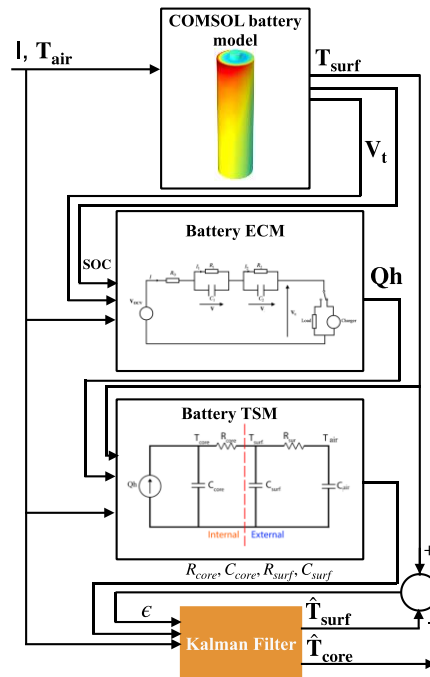


Figure. Schematic diagram summarising the battery core temperature estimation process

Aim

Provide an accurate estimation of the battery core temperature considering the non-uniform temperature distribution.

Design & Methodology

Thermal parameter identification of Li-ion battery using recursive least squares algorithm and core temperature estimation using Kalman filter method.

Originality

Using the COMSOL Software to monitor the unmeasurable quantities of the battery and use the acquired data for an accurate representation of the battery's thermal behaviour.

Findings

The proposed TSM has an estimation error of $3,8 \cdot 10^{-3} \text{ K}$ and a 0.037 RMSE for the estimated core temperature at an initial condition of 298,15 K under the UDDS drive cycle.

Conclusion

As a crucial factor that influences the battery's safety and life cycle, we were able to model its thermal behaviour and estimate its core temperature accurately to prevent thermal runaway.

Declaration of Ethical Standards

The author(s) of this article declare that the materials and methods used in this study do not require ethical committee permission and/or legal-special permission.

Li-Ion Battery Thermal Parameter Identification and Core Temperature Estimation

Araştırma Makalesi / Research Article

Khadija SAQLI^{1*}, Houda BOUCHAREB¹, Mohammed OUDGHIRI¹, Nacer Kouider M'SIRDI²

¹LISAC, Sidi Mohamed Ben Abdellah University, Fez, Morocco

²LSIS, Aix-Marseille University, Marseille, France

(Geliş/Received : 15.08.2022 ; Kabul/Accepted : 27.10.2022 ; Erken Görünüm/Early View : 27.11.2022)

ABSTRACT

Battery core and surface temperature are crucial for the thermal management and safety usage of Li-ion batteries. They affect the cell's physical properties and strongly correlate with some of its key states, such as the battery state of charge (SOC) and state of health (SOH). Therefore, an accurate estimate of the battery core and surface temperature will enhance the performance and prolong the battery's life. This study proposes an estimation system of the battery core and surface temperature. A simplified pseudo-two-dimensional model is introduced to capture the battery SOC, core and surface temperature that will be used later in this study to model and validate the results' accuracy. Then, a two-state thermal battery model (TSM) is presented and studied. The recursive least square (RLS) algorithm is adopted to identify the thermal parameters of the battery. Next, the TSM is validated using COMSOL Multiphysics simulation software and the thermal parameters are then fed to the Kalman filter (KF) to estimate the battery core temperature. Finally, the accuracy of the battery core temperature estimated results are validated with a root mean square error of 0.037K.

Keywords: Li-ion battery thermal model, core temperature, surface temperature, kalman filter, recursive least squares.

Li-Ion Pil Termal Parametre Tanımlama ve Çekirdek Sıcaklık Tahmini

ÖZ

Pil çekirdeği ve yüzey sıcaklığı, Li-ion pillerin termal yönetimi ve güvenli kullanımı için çok önemlidir. Onlar, hücrenin fiziksel özelliklerini etkilerler ve pil şarj durumu (SOC) ve sağlık durumu (SOH) gibi bazı temel durumları ile güçlü bir korelasyona sahiptirler. Bu nedenle, pil çekirdeğinin ve yüzey sıcaklığının doğru bir tahmini, performansı artıracak ve pilin ömrünü uzatacaktır. Bu çalışma, pil çekirdeği ve yüzey sıcaklığı için bir tahmin sistemi önerilmektedir. Pil SOC'sini, çekirdek ve yüzey sıcaklığını yakalamak için basitleştirilmiş bir sözde iki boyutlu model tanıtılmış, sonrasında bu çalışmada elde edilen sonuçları doğrulamak ve modellemek için kullanılmıştır. Ardından, iki durumlu bir termal pil modeli (TSM) sunulmuş ve incelenmiştir. Pilin termal parametrelerini tanımlamak için öz yinlemeli en küçük kareler (RLS) algoritması benimsenmiştir. Daha sonra, TSM; COMSOL Multiphysics simülasyon yazılımı kullanılarak doğrulanmış ve sonrasında termal parametreler, pil çekirdek sıcaklığını tahmin etmek için Kalman filtresine (KF) uygulanmıştır. Sonuç olarak, pil çekirdek sıcaklığı tahmini sonuçlarının doğruluğu 0.037K'lık bir ortalama karekök hatasıyla doğrulanmıştır.

Anahtar Kelimeler: Li-ion pil termal modeli, çekirdek sıcaklığı, yüzey sıcaklığı, kalman filtresi, öz yinlemeli en küçük kareler

1. INTRODUCTION

Nowadays, Lithium-ion batteries (LIBs) have become the beating heart of portable electronics and electric vehicles (EVs) thanks to their high energy density, lightweight and no memory effects. Nevertheless, they are susceptible to temperature variations. For optimal performance, LIB must operate at a controlled temperature between 15 °C – 35 °C [1,2]. Both low and high temperatures outside this optimum range will promote battery ageing and cause lithium plating and thermal runaway. A primary concern of the thermal management system is the estimation of the battery temperature. Generally, LIBs are packed in series and/or

parallels to achieve the required capacity and voltage. During operation, li-ion cells release heat due to enthalpy changes, electrochemical polarization and resistive heating [3]. The accumulated heat may lead to local overheating and thus local deterioration of the battery pack. Li-ion temperature is defined by its core and surface temperature. To measure the battery core temperature, we can use an embedded thermocouple inside the cell. This approach is costly and not practical, especially for large battery packs where we need to control and capture the core temperature for each cell. Therefore, accurate estimation of the battery core and surface temperature is crucial for battery management systems along with the battery state of charge (SOC), state of health (SOH), and other essential states for safe and reliable performance.

*Sorumlu Yazar (Corresponding Author)
e-posta : khadija.saqli@usmba.ac.ma

Modelling allows a better understanding of how the battery responds to load. The accuracy of the proposed model is judged based on how well it performs under different thermal conditions and its efficiency. The literature presents various battery models with diverse ranges of complexity and accuracy and can be grouped into two categories: heat generation and heat transfer models [4]. The first category (heat generation models) takes the cell current as input to describe the battery behavior and estimate the total heat generation during operation. It usually includes electrochemical battery models (EM) and equivalent circuit models (ECM). As the name implies, ECM uses electrical components to procreate the cell response. It usually includes an open circuit voltage to describe the internal battery voltage, a series resistance representing the Ohmic drop, and one or multiple RC blocks describing the polarization effect caused by diffusion, transfer or other effects [5]. Due to their simplicity and acceptable accuracy, ECMs are the model of choice for model-based estimation methods [6]. However, their precision is subject to the identified model parameters, temperature ageing and other factors.

On the other hand, EMs describe the internal microscopic quantities that the electric models can't capture, which makes them suitable for battery degradation analysis [7]. EMs can be grouped into three main categories: pseudo-two-dimensional (P2D) models, single particle (SP) models, and simplified P2D (SP2D) models. Each model has its limitation and advantages. The P2D was first established by M. Doyle, T. F. Fuller and J. Newman [8]. It uses partial differential equations (PDEs) to describe the reaction kinetics, migration and diffusion inside the Li-ion cell [7]. The PDEs have no analytic solutions. Thus, specific discretization methods are used to solve them [11]. The full P2D model is complex and requires heavy computational power making them unsuitable for real-time applications. On the other hand, the SP model is a simplified version that assumes each electrode to be modelled by a single spherical particle, which reduces the PDEs system to less than ten states. This simplification reduces the accuracy of the model but speeds up the computation. The SP2D battery model is derived from the P2D and inherits its accuracy with reduced computational burden. Heat transfer models use the heat estimated by the heat generation model to calculate the cell core and surface temperature. They can be classified into finite element analysis (FEA) [13, 14] and heat capacitor-resistor models [12], each with advantages and drawbacks. Unlike FEA-based models [13], the heat capacitor-resistor models are more straightforward and computationally inexpensive. They can be optimized to improve the estimation accuracy, making it the choice model for several real-world management systems.

Heat capacitor-resistor models apply the analogy between thermal and electrical phenomena to describe the thermal behaviour of the battery when a load is applied. Researchers have introduced different heat capacitor-resistor models with various accuracy and complexity levels. These models can be broadly

classified into two main categories: first-order and second-order based thermal models [12-14]. Compared to second-order models that require extensive experiments and the profound knowledge of domain experts, first-order models are more straightforward and reasonably accurate. Thus, determined efforts were employed to overcome these shortcomings [13].

Different approaches were used to estimate the core temperature of LIBs. The most common method is the electrochemical-impedance-spectroscopy (EIS) based method. Robert R. et al. [15] used the EIS measurements combined with the surface temperature measurements to estimate the battery's internal temperature. Despite its accuracy, finding the appropriate frequency of the EIS is complex and can be acquired through tedious preliminary tests.

Data-driven models are widely used to forecast battery performance based on a dataset. In [16], Kleiner et al. proposed a unique NARX network for a 25 Ah hexagonal cell to predict the battery's thermal behaviour. The model uses real-life datasets to make predictions of internal temperature. However, the focus is on thermal causes over the battery lifespan, as opposed to more complex real-world situations that may have different consequences. To include the interdependency between the battery's electrical and thermal behaviour, Konglei et al. [17] proposed an enhanced EIS-based core temperature estimation approach. The model quantitatively selects the SoC-insensitive EIS features to be used by the support vector regression (SVR) to improve the temperature prediction. However, the data-driven artificial neural network methods have been mainly employed to estimate the battery SOC [18-20] and SOH [21-23] and are less adapted for temperature-states estimation. An adaptive observer is applied in [24, 25] to assess the internal temperature of the LIB in a battery pack. The estimation errors are fed back to adopt the prediction. This approach is used in various studies to estimate the battery cell's core temperature by measuring the cell's surface temperature. The main drawback of this estimation category is that it requires several temperature sensors to improve observability, especially for large-scale battery packs. In [26], Jiang Yu Hen et al. used two types of neural networks: long short-term memory-RNN (LSTM-RNN) and gated recurrent unit-RNN (GRU-RNN) to estimate the battery surface temperature. However, the performance of neural network-based methods is greatly affected by the training iteration and overfitting, making the estimation more challenging.

Estimating the battery core temperature is essential for thermal management and assessing temperature distribution. A sure and effective estimation algorithm of the battery core temperature will improve the battery performance. In recent studies [27, 28], Kalman filter (KF) has been widely used to predict the battery core temperature and the battery states. The algorithm is known for its robustness and was proven its ability to provide accurate estimation, even under noisy operating conditions. Therefore, KF was chosen for this study to

estimate the battery's internal temperature based on the two-state thermal model.

The main goal of this study is to provide a platform that can monitor the battery temperature during operation and guarantee its safety. The proposed model considers the non-uniform temperature distribution inside the battery to achieve a real-time estimation of the battery core temperature. The battery cell is first simulated in COMSOL Multiphysics to extract the necessary data needed to develop the thermal battery model and validate its accuracy. The simulated model captures the battery core and surface temperature, the generated heat, the coolant air temperature and the lithium concentration in the electrode to measure the SOC variation under the load.

The paper is organized as follows: Section 2 introduces the methods used in this study to model the thermal characteristics of the battery and track the lithium concentration evolution during operation to estimate its SOC. Section 3 presents the data acquired from the CFD simulation, the estimated thermal parameters of the LMO battery using this data and the core temperature estimation results under the CC test using the KF approach. Finally, we conclude our work in section 4.

2. METHODS

Generally, Li-ion batteries are available in three major form factors: cylindrical cells, pouch cells and prismatic cells. Each geometry is better suited to different use cases. Cylindrical cells have proven to be most adaptable for high-power applications thanks to their high specific energy and good mechanical stability. However, the jellyroll shape of the battery causes a significant temperature difference between the core and the surface. Thus, it's essential to provide a thermal model of the battery to predict its core temperature for effective thermal management.

2.1. Electrochemical Model

The electrochemical battery model is set up using the physics interface "Lithium-Ion Battery" in COMSOL Multiphysics. The model is developed and validated based on the work of Newman, Fuller and Doyle [8-10]. It uses well-proven electrochemical and thermodynamic concepts to describe the inner behaviour of the battery during operation. The high performance and accuracy of the model pushed its use as a reference for validation by the Li-ion battery modelling community [29]. Therefore, it was chosen to parametrise and validate the thermal model of the 18650 cylindrical graphite/LMO Li-ion cell (Figure 1) to accurately estimate the core temperature while considering the noise and the inner electrical resistance of the battery.

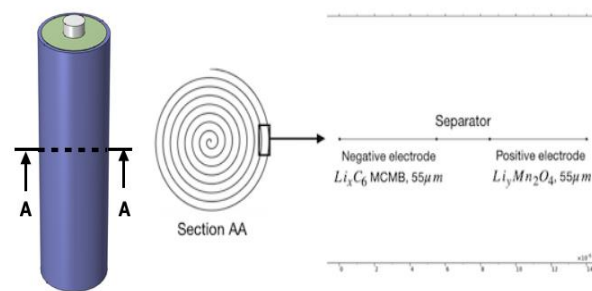


Figure 1. The LMO 18650 battery geometry

As shown in Figure 1, the cylindrical cell is built by alternating the positive electrode, the separator and the negative electrode. The current collector at the positive and negative end of the battery accumulates the generated current. The governing PDEs are thoroughly presented in our previous work [30] and won't be represented here for simplicity. We upgraded the earlier model of [30] to capture the battery core and surface temperature, the temperature of the air flowing inside the compartment, the battery SOC and the generated heat. The properties of the battery are listed in Table 1.

Table 1 Battery properties

Battery properties	Value
Diameter (mm)	18
Height(mm)	56
Chemistry	Li-ion manganese oxide (LMO)
Heat capacity (J/(Kg.K))	1399.1
Radial thermal conductivity (W/(m.K))	0.89724

2.1.1. SOC and Lithium Concentration

Battery SOC is a crucial measurement that affects the energy management control strategy and performance [31]. It describes the amount of charge left relative to its initial capacity under a current load. An accurate estimation of this state helps prevent overcharging and over-discharging the battery cell for safe and prolonged life usage. For electrochemical battery models, the battery SOC can be defined as in [29]

$$SOC = \frac{\int_{\Omega_n} c_{s,surf,cycl} F \epsilon_s d\Omega}{\int_{\Omega_n} c_{s,surf,cycl} F \epsilon_s d\Omega + \int_{\Omega_p} c_{s,surf,cycl} F \epsilon_s d\Omega} \quad (1)$$

Where the spatial domain $\Omega \subset \mathbb{R}^N$, F is Faraday's constant, ϵ_s is the electrode volume fraction and $c_{s,surf,cycl}$ is the cyclable lithium concentration at the surface of the electrode particles defined as

$$c_{s,surf,cycl} = c_{s,surf} - soc_{min} c_{s,max} \quad (2)$$

Where $c_{s,surf}$ represents the lithium concentration at the surface of the electrode particles and soc_{min} and $c_{s,max}$ represent respectively the electrode minimum state of charge and the maximum solid phase concentration.

2.1.2. Temperature and Heat Generation

Since the 18650 cylindrical cells are usually used in large-scale high-power applications, they are subject to temperature rise due to the generated heat in the primary reaction and unwanted side reactions. Heat can originate from resistive dissipation, the entropy of the cell reaction, the heat of mixing, and side reactions [32].

The heat and temperature equation applied to the cell is given as

$$\rho C_p \frac{dT(x,t)}{dt} = \lambda_i \frac{dT(x,t)}{dx^2} + Q_{ohm}(x,t) + Q_{rev}(x,t) + Q_{rxn}(x,t) \quad (3)$$

The total irreversible ohmic heat generation rate

$$\begin{aligned} Q_{ohm}(x,t) &= \sigma_{eff} \left(\frac{\partial \Phi_s(x,t)}{\partial x} \right)^2 \\ &+ \kappa_{eff} \left(\frac{\partial \Phi_e(x,t)}{\partial x} \right)^2 \\ &+ \frac{2RT(x,t)}{F} \kappa_{eff} \left(1 - t_+ \right) \frac{\partial \ln(c_e(x,t))}{\partial x} \frac{\partial \Phi_e(x,t)}{\partial x} \end{aligned} \quad (4)$$

The total reversible heat generation rate

$$Q_{rev}(x,t) = a_i F J(x,t) T(x,t) \frac{\partial U(x,t)}{\partial T} \quad (5)$$

The total irreversible heat generation rate

$$Q_{rxn}(x,t) = a_i F J(x,t) \eta_i(x,t) \quad (6)$$

where ρ , C_p , λ , σ_{eff} , κ_{eff} define respectively the density, the heat capacity, the conduction coefficient, the effective conductivity and the specific conductivity of the electrolyte. t_+ is the transference number of lithium ions, a_i is the electrode surface area per volume unit of the electrode, J is the flux of lithium ions flowing out of the surface of the spherical particles and η_i is the resulting overpotential.

The boundary conditions are defined as

$$\begin{cases} \left[-\lambda_i \frac{\partial T(x,t)}{\partial x} \right]_0 = h(T_{ref} - T(x,t)), \\ \left[-\lambda_i \frac{\partial T(x,t)}{\partial x} \right]_L = h(T_{ref} - T(x,t)) \end{cases} \quad (7)$$

where h is the convection coefficient, T_{ref} is the ambient temperature.

Finally, we can define the thermal dependence open circuit voltage (OCV) using Taylor's first order expansion around a reference temperature as

$$U_p = U_{p,ref} + (T(x,t) - T_{ref}) \left. \frac{\partial U_p}{\partial T} \right|_{T_{ref}} \quad (8)$$

$$U_n = U_{n,ref} + (T(x,t) - T_{ref}) \left. \frac{\partial U_n}{\partial T} \right|_{T_{ref}}$$

where $U_{p,ref}$ and $U_{n,ref}$ represent respectively the OCV at the positive and negative electrode under reference temperature T_{ref} and $\left. \frac{\partial U_p}{\partial T} \right|_{T_{ref}}$, $\left. \frac{\partial U_n}{\partial T} \right|_{T_{ref}}$ is the entropy change of the positive and negative electrode respectively.

2.2. Thermal Model

The accuracy of the thermal estimator depends mainly on the selected thermal battery model. Thus, a two-state thermal battery model (TSM) was selected in this study to describe the battery inner and outer thermal behavior. As shown in Figure 2, the model includes the heat generated by the battery core during operation Qh , the heat capacity of the core C_{core} , the battery core heat transfer resistance R_{core} , the thermal capacitance of the battery canister C_{surf} and the thermal heat resistance of the battery surface R_{surf} .

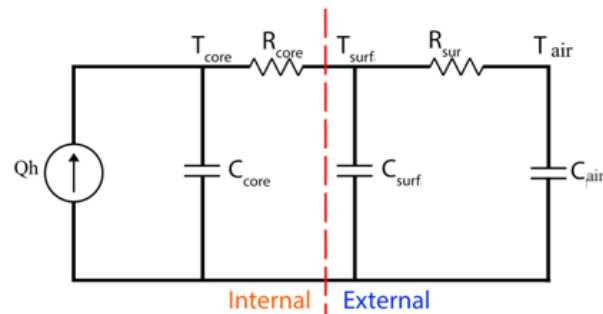


Figure 2. Two-state thermal battery model

The model equations are defined according to the law of conservation of energy as

$$C_{core} \frac{dT_{core}}{dt} = Qh + \frac{T_{surf} - T_{core}}{R_{core}} \quad (9)$$

$$C_{surf} \frac{dT_{surf}}{dt} = \frac{T_{air} - T_{surf}}{R_{surf}} - \frac{T_{surf} - T_{core}}{R_{core}} \quad (10)$$

Where T_{core} , T_{surf} represent respectively the battery core temperature and surface temperature.

The heat generation rate Qh adopts the Bernardi heat generation model [33] and can be acquired as follow

$$Qh = (OCV - V_t)I_{app} - IT \frac{dU_{ocv}}{dT} \quad (11)$$

Where **OCV** is the battery open circuit voltage, V_t defines the battery terminal voltage, I_{app} is the input current $\frac{dU_{ocv}}{dT}$ represent the entropy heat coefficient.

2.2.1. Parameter Identification

By combining the temperature dependent second order equivalent circuit model that we developed in a previous work [30] with this TSM battery model we can calculate the battery heat generation using equation 11. The entropy heat coefficient was ignored since the temperature impact on the OCV change is minor. Thus, only the irreversible heat is considered.

$$z(k) = \theta^T \phi(k) \quad (12)$$

Where $z(k) = T_{surf}(k)$ is the model input, $\phi(k) = [T_{surf}(k), T_{air}(k-1), T_{air}(k), Qh]^T$ is the identified related parameters and θ is the model output. equations 9 and 10 are discretized as

$$T_{surf}(k) = \frac{R_{surf}}{R_{surf} + R_{core}} T_{core}(k) + \frac{R_{core}}{R_{surf} + R_{core}} T_{air}(k) \quad (13)$$

$$T_{core}(k-1) = \frac{R_{surf} + R_{core}}{R_{surf}} T_{surf}(k-1) - \frac{R_{core}}{R_{surf}} T_{air}(k-1) \quad (14)$$

By sorting out equation 13 and 14 we get

$$T_{surf}(k) = \frac{R_{core}C_{core} + R_{surf}C_{core} - \Delta t}{C_{core}(R_{core} + R_{surf})} T_{surf}(k-1) - \frac{\Delta t - R_{core}C_{core}}{C_{core}(R_{core} + R_{surf})} T_{air}(k-1) + \frac{R_{core}}{R_{surf} + R_{core}} T_{air}(k) + \frac{R_{surf}\Delta t}{C_{core}(R_{core} + R_{surf})} Qh(k-1) \quad (15)$$

We set

$$\left\{ \begin{aligned} \alpha_1 &= \frac{R_{core}C_{core} + R_{surf}C_{core} - \Delta t}{C_{core}(R_{core} + R_{surf})} \\ \alpha_2 &= \frac{\Delta t - R_{core}C_{core}}{C_{core}(R_{core} + R_{surf})} \\ \alpha_3 &= \frac{R_{core}}{R_{surf} + R_{core}} \\ \alpha_4 &= \frac{R_{surf}\Delta t}{C_{core}(R_{core} + R_{surf})} \end{aligned} \right.$$

Where Δt is the sampling time and was set to 1s and $\theta = [\alpha_1, \alpha_2, \alpha_3, \alpha_4]$ represent the model parameters to be identified.

2.2.2. Core Temperature Estimation using KF

The main focus of this section is to use the identified thermal parameters of the 18650 LMO LIB to estimate its core temperature using Kalman filter (KF).

KF algorithm is an effective and well-known algorithm widely used to estimate the states of a linear dynamic system. Due to its high accuracy and good performance even with noisy measurements, KF is chosen in this study to evaluate the battery core and surface temperature.

A schematic diagram of the battery core and surface estimation is illustrated in Figure 3. The diagram inputs are the inlet air temperature T_{air} used to dissipate the generated heat during operation, and the applied current I . The RLS algorithm uses the model inputs and the surface temperature obtained from the CFD simulation to identify the thermal parameters of the TSM including C_{core} , R_{core} , C_{surf} and R_{surf} needed for the KF algorithm to estimate the battery core and surface temperature. The surface temperature estimated by the KF is compared to that of the CFD simulation and the generated estimation error is then used to calibrate the KF.

Herein we define the state space vector as $x = [T_{core}, T_{surf}]$, the system output as $y = T_{surf}$ and the $u = [I, T_{air}]$.

$$\begin{cases} x(k+1) = Ax(k) + Bu(k) + \omega \\ y(k) = Cx(k) + v \end{cases} \quad (16)$$

ω and v are the uncorrelated Gaussian variable. The matrix coefficients A and B are derived from equation 9 and 10 as

$$A = \begin{bmatrix} 1 - \frac{\Delta t}{C_{core}R_{core}} & \frac{\Delta t}{C_{core}R_{core}} \\ \frac{\Delta t}{C_{surf}R_{core}} & 1 - \frac{\Delta t}{C_{surf}R_{surf}} - \frac{\Delta t}{C_{surf}R_{core}} \end{bmatrix} \quad (17)$$

$$B = \begin{bmatrix} \frac{\Delta t}{C_{core}} & 0 \\ 0 & \frac{\Delta t}{C_{surf}R_{surf}} \end{bmatrix}$$

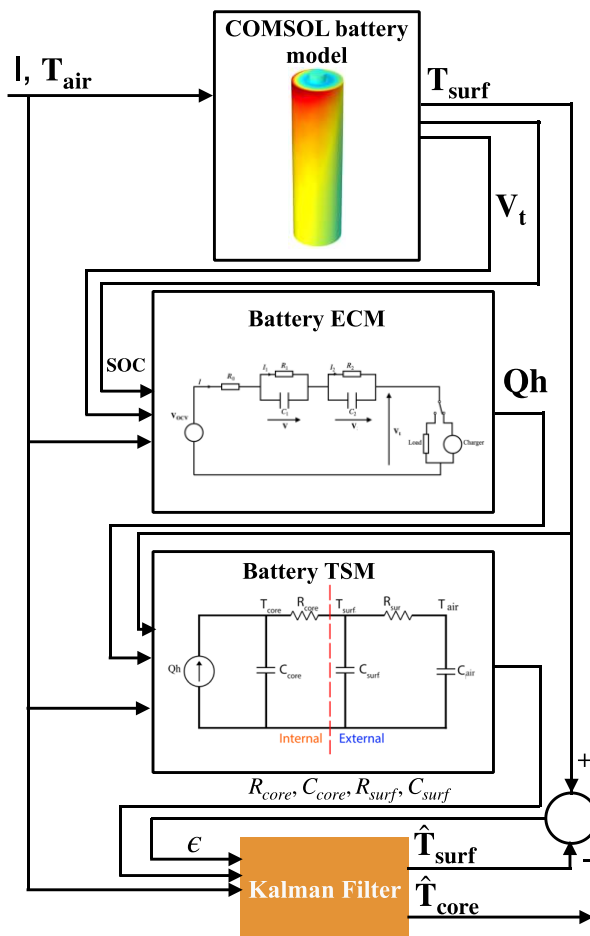


Figure 3 Schematic diagram of the battery core temperature estimation process

3. RESULTS AND DISCUSSION

This section presents the simulation results as well as the validation of the TSM battery model and the core temperature estimation results using the KF algorithm.

3.1. Simulation Results of the Electrochemical Battery Model

The battery is placed in a compartment where air flows with an inlet velocity of $v_{in} = 0.1$ m/s and an initial temperature of $T_{air,0} = 298.15$ K to simulate a thermal chamber. We start with a fully charged battery $SOC = 100\%$ and $V_0 = 4.2$ V, and we apply a 1C (-12Ah) constant current charge (see Figure 4) to bring the cell's SOC to 2%.

The 1D cell model was built and validated by COMSOL Multiphysics. The 1D and 3D are linked using a coupling function of the cell temperature and the generated heat. The cell and the air compartment are meshed using physics-controlled mesh to simulate the cell and the cooling air.

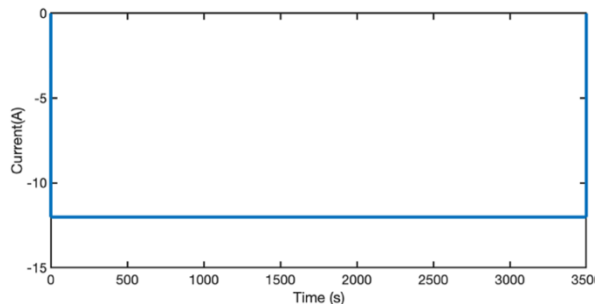


Figure 4. Discharge current load

To avoid over-discharging the battery cell, we applied a 1C-rate current load for 3500s, and we stopped when $SOC = 2\%$. The simulation results are shown in Figure 5 and will be later used to estimate the battery core and surface temperature.

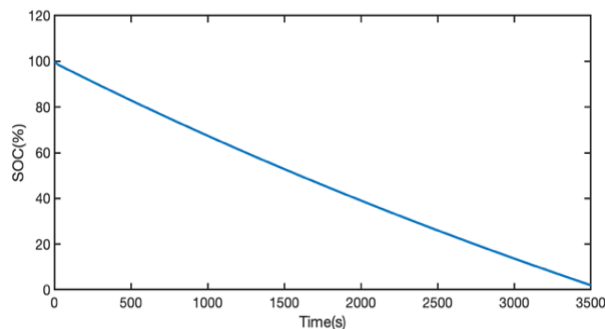


Figure 5. Battery SOC

The core, surface and air temperature measured under the CC load are illustrated in Figure 6 and will be used as experimental results to calculate the battery thermal model parameters and validate later on the estimation results of the core temperature using Kalman filter with the identified parameters. It can be seen that the battery core temperature is slightly higher than the surface temperature. This is due to the air flowing inside the compartment to cool the cell and reduce the temperature gradient. The air, core and surface temperature reached its maximum value of 300.7K at the end of the simulation without exceeding the permissible thermal limits for safe operation, and this is due to the effective thermal management.

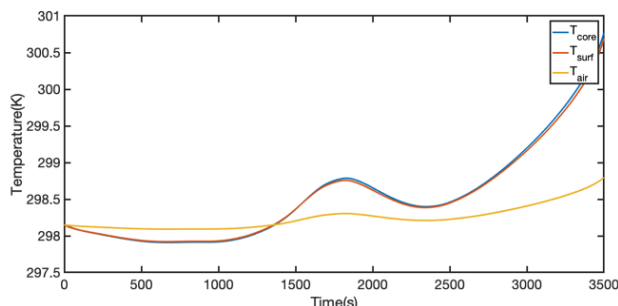


Figure 6. Simulation results of the battery core, surface and air temperature for parameter identification

During discharge, the crystal phase transition from hexagonal to monoclinic of the cathode material of the LMO battery leads to endothermic heat effect, which explains the distinct drop in the battery temperature near 2400 s.

3.2. Thermal Parameters Estimation Results

To test the RLS algorithm and estimate the TSM parameters including C_{core} , R_{core} , R_{surf} , we used the data that we acquired from the SP2D model.

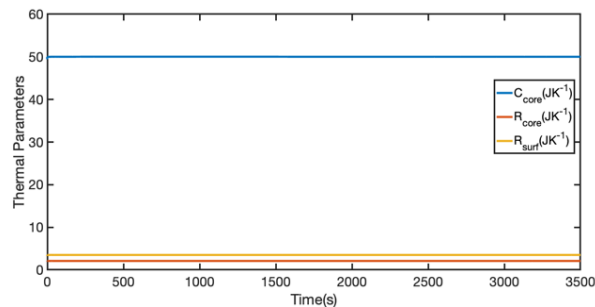


Figure 7. Battery thermal parameters identification results

As illustrated in Figure 7, The battery thermal parameters do not change with the physical properties of the cell and thus can be identified as constants. We can acquire the battery surface heat capacity (C_{surf}) from the heat capacity and the size of the battery canister. Therefore, only the other three parameters can be identified using the RLS algorithm. Finally, the estimated thermal parameters of the TSM model are listed in Table 2.

Table 2. Battery thermal parameters

Thermal parameters	Value	95% confidence interval
$C_{core}(JK^{-1})$	50.0162	50.0158 - 50.0166
$C_{surf}(JK^{-1})$	3.42	-
$R_{core}(JK^{-1})$	2.104	2.1039 - 2.1041
$R_{surf}(JK^{-1})$	3.5067	3.5065 - 3.5069

To validate the accuracy of the TSM battery model, we used the identified thermal parameters to calculate the surface temperature, and we compared it to the surface temperature acquired from the CFD simulation. The results are shown in Figure 8.

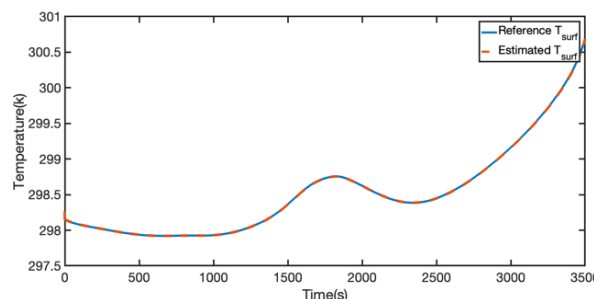


Figure 8. Comparison of the battery reference and estimated surface temperature using the identified TSM model

The estimation root means square errors of the battery surface temperature using the estimated thermal parameters is $3.8 \cdot 10^{-3} \text{ K}$, which proves the accuracy of

the developed TSM to predict the thermal behavior of the battery.

3.3. Core and Surface Temperature Estimation Results

To investigate the performance of the KF algorithm, we set the simulated core and surface temperature under the CC test obtained from the CFD simulation as reference data upon which we compare the results of the KF.

The state initial value is set as $x = [298.15, 298.15]$ the air temperature $T_{air} = 298.15K$, the inlet velocity $v_{in} = 0.1m/s$ and sampling time $\Delta t = 1s$.

Figure 9 shows comparison of the estimated core temperature and reference temperature at (a) 298.15 K, (b) 303.15. K, (c) 316.15. K. The results show that the core and surface temperature acquired from the KF algorithm are in good accord with the reference values. For 298.15 K, the errors of the core temperature are kept between $-0.014 K$ and $0.13 K$ with a RMSE of $0.037 K$, which proves the accuracy of the proposed model to predict with high confidence the thermal behavior of the li-ion battery.

outside the optimum range of operation and with poor thermal management system, the proposed estimation scheme accurately predicted the battery's thermal behavior.

3. CONCLUSION

Battery temperature, be it core or surface temperature, is a crucial factor influencing battery Safety and other parameters such as the battery SOC and SOH. Monitoring the battery core and surface temperature is essential for thermal management. Thus, the focus of this study was to study and model first the thermal behavior of the 18650 LMO battery cell and present a reliable estimate of the battery core temperature based on KF. We started by acquiring the essential data needed for the identification process of the TSM and the estimation algorithm, using the SP2D battery model. Next, we applied the RLS algorithm to identify the TSM parameters, including C_{core} , C_{surf} , R_{core} , R_{surf} , and R_{core} . The surface temperature estimated using the identified thermal parameters has an estimation error of $3.8 \cdot 10^{-3} K$, proving the developed TSM to track the

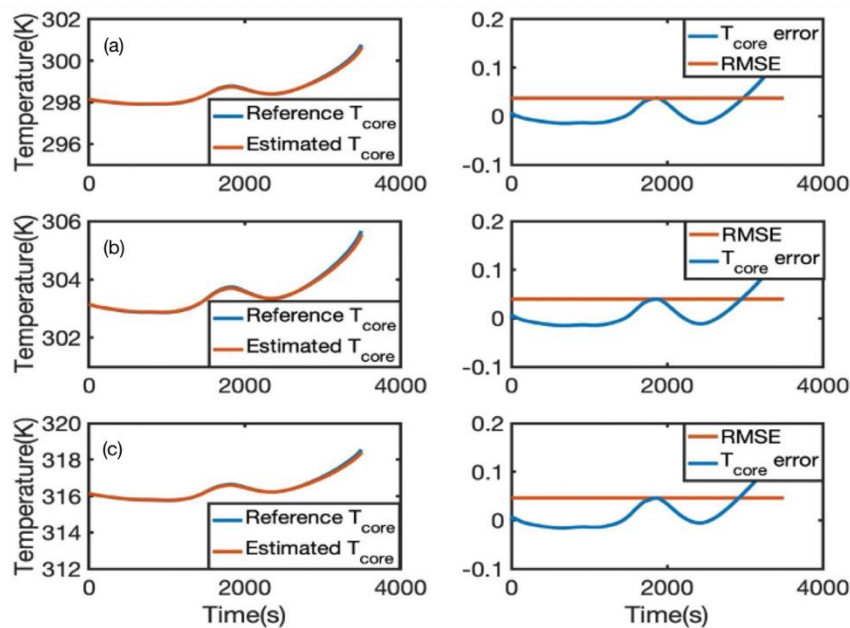


Figure 9. Estimation results of the battery core temperature using KF at (a) 298.15K, (b) 303.15 K and (c) 316.15 K

To investigate the impact of temperature on the accuracy and performance of the developed model, we compared the core temperature simulated by the SP2D battery model to the core temperature estimated by the proposed model at different range of temperatures. We set the coolant air temperature to match the ambient temperature during the test to decrease its impact on the battery thermal response. At 303,15K, the core temperature estimation errors are between $-0,01 K$ and $0,13 K$. At the end of the simulation, the battery's core temperature increased by $2.39 K$. At 316,15 K, the model was able to accurately estimate the battery core temperature with an RMSE of $0.046 K$. Even at elevated temperatures that's

battery's thermal behaviour with high accuracy. Finally, we applied KF to estimate the battery core temperature. The results show good accordance between the estimated and the reference core temperature with RMSE of $0.037 K$ for an initial temperature of $298.15 K$, which proves the accuracy of the developed thermal model and the estimator. The performance of the TSM model was tested at an extreme operating condition of $303.15 K$ and $316.15 K$. At $303,15K$ the battery core temperature estimation errors were between $- 0,01 K$ and $0,13 K$, while for $316.15 K$ the estimated core temperature has an RMSE of $0.046 K$. These results revealed the ability of the proposed TSM with the KF algorithm to provide sturdy

results even under elevated temperatures that exceed the optimum range of operation.

DECLARATION OF ETHICAL STANDARDS

The author(s) of this article declare that the materials and methods used in this study do not require ethical committee permission and/or legal-special permission.

AUTHORS' CONTRIBUTIONS

Khadija SAQLI: Performed the experiments, analysed the results and wrote the manuscript.

Houda BOUCHARB: Proofread the manuscript.

Oudghiri Mohammed: Directed the study and proofread the manuscript.

Nacer Kouider M'SIRDI: Directed the study and proofread the manuscript.

CONFLICT OF INTEREST

There is no conflict of interest in this study

REFERENCES

- [1] Mahfoudi, N., Boutaous, M., Xin, S., Buathier, S., "Thermal Analysis of LMO/Graphite Batteries Using Equivalent Circuit Models", *Batteries*, 7, 58, 2021.
- [2] Chen, D., Jiang, J., Kim, G., H., Yang, C., Pesaran, A., "Comparison of different cooling methods for lithium-ion battery cells", *Applied Thermal Engineering*, 94, 846-854, 1359-4311, (2016).
- [3] Ismail, N.H.F., Toha, S.F., Azubir, N.A.M., Ishak, N.H.M., Hassan, I.D.M.K., Ibrahim, B.S.K., "Simplified heat generation model for lithium-ion battery used in electric vehicle", *IOP Conference Series: Materials Science and Engineering*, 53: 012014, (2013).
- [4] Pan, Y. W., Hua, Y., Zhou, S., He, R., Zhang, Y., Yang, S., Liu, X., Lian, Y., Yan, X., Wu, B., "A computational multi-node electro-thermal model for large prismatic lithium-ion batteries", *Journal of Power Sources*, 459: 228070, (2020).
- [5] Ko, S. T., Ahn, J. H., Lee, B.K., "Enhanced equivalent circuit modeling for li-ion battery using recursive parameter correction", *Journal of Electrical Engineering and Technology*, 13: 1147-1155, (2018).
- [6] He, W., Pecht, M.G., Flynn, D., Dinmohammadi, F., "A Physics-Based Electrochemical Model for Lithium-Ion Battery State-of-Charge Estimation Solved by an Optimised Projection-Based Method and Moving-Window Filtering", *Energies*, 11, 8: 2120, (2018).
- [7] Zhou, J., Xing, B., Wang, C. "A review of lithium ion batteries electrochemical models for electric vehicles", *E3S Web of Conferences*, 185: 04001, (2020).
- [8] Doyle, M., Thomas F. F., Newman J., "Modeling of Galvanostatic Charge and Discharge of the Lithium/Polymer/Insertion Cell", *Journal of The Electrochemical Society*, 140(6): 1526, (1993).
- [9] Fuller, T. F., Doyle, M., Newman, "Simulation and Optimization of the Dual Lithium Ion Insertion Cell," *Journal of the Electrochemical Society*, 141, 1, 1-10, 1994.
- [10] Fuller, T. F., Doyle, M., Newman, "Relaxation Phenomena in Lithium-Ion-Insertion Cells", *Journal of The Electrochemical Society*, 141, 982, (1994).
- [11] Kemper P., Li S.E., Kum D., "Simplification of pseudo two-dimensional battery model using dynamic profile of lithium concentration", *Journal of Power Sources*, 286: 510-525, (2015).
- [12] Damay, N., Forgez, C., Bichat, M.-P., & Friedrich, G., "Thermal modeling of large prismatic LiFePO₄/graphite battery. Coupled thermal and heat generation models for characterization and simulation", *Journal of Power Sources*, 283: 37-45, (2015).
- [13] Saw, L. H., Poon, H. M., Thiam, H. S., Cai, Z., Chong, W. T., Pambudi, N. A., King, Y. J., "Novel thermal management system using mist cooling for lithium-ion battery packs", *Applied Energy*, 223: 146-158, (2018).
- [14] Liu, B., Yin, S., Xu, J., "Integrated computation model of lithium-ion battery subject to nail penetration", *Applied Energy*, 183: 278-289, (2016).
- [15] Richardson, R. R., Ireland, P. T., Howey, D. A., "Battery internal temperature estimation by combined impedance and surface temperature measurement", *Journal of Power Sources*, 265: 254-261, (2014).
- [16] Kleiner, J., Stuckenberger, M., Komsijska, L., Endisch, C., "Real-time core temperature prediction of prismatic automotive lithium-ion battery cells based on artificial neural networks", *Journal of Energy Storage*, 39: 102588, 2352-152X, (2021).
- [17] Konglei, O., Yuqian, F., Mohammad, Y., Weiwen, P., "Data-driven Based Internal Temperature Estimation for Lithium-ion Battery Under Variant SoC via Electrochemical Impedance Spectroscopy", *Energy Technol*, 10: 2100910, (2022).
- [18] Ismail, M., Dlyma, R., Elrakaybi, A., Ahmed, R., Habibi, S., "Battery state of charge estimation using an Artificial Neural Network," *2017 IEEE Transportation Electrification Conference and Expo (ITEC)*, 342-349, (2017).
- [19] Kuchly, J., Goussian, A., Merveillaut, M., Baghdadi, I., Franger, S, Nelson-Gruel, D., Nouillant, C., Chamailard, Y., "Li-ion battery SOC estimation method using a Neural Network trained with data generated by a P2D model", *IFAC-PapersOnLine*, 54, 10, 336-343, 2405-8963, (2021).
- [20] Charkhgard, M., Farrokhi, M., "State-of-Charge Estimation for Lithium-Ion Batteries Using Neural Networks and EKF", *IEEE Transactions on Industrial Electronics*, 57, 12, 4178-4187, (2010).
- [21] Li, Q., Li, D., Zhao, K., Wang, L., Wang, K., "State of health estimation of lithium-ion battery based on improved ant lion optimization and support vector regression", *Journal of Energy Storage*, 50, 104215, 2352-152X, (2022).
- [22] Inioluwa, O., Chikodinaka. E., "State of Health Estimation of Lithium-Ion Batteries Using Support Vector Regression and Long Short-Term Memory", *Open Journal of Applied Sciences*, 12, 1366-1382, (2022).
- [23] Lee, G., Kim, J., Lee, C., "State-of-health estimation of Li-ion batteries in the early phases of qualification tests: An interpretable machine learning approach", *Expert Systems with Applications*, 197, 116817, 0957-4174, (2022).
- [24] Liu, Z., Du, J., Stimming, U., Wang, Y., "Adaptive observer design for the cell temperature estimation in battery packs in electric vehicles", *2014 IEEE 9th*

- Conference on Industrial Electronics and Applications (ICIEA 2014)*; IEEE: Hangzhou, China, 348–353, (2014).
- [25] Lin, X., Fu, H., Perez, H.E., Siegel, J.B., Stefanopoulou, A.G., Ding, Y., Castanier, M.P., “Parameterization and Observability Analysis of Scalable Battery Clusters for Onboard Thermal Management”. *Oil & Gas Science and Technology Revue d’IFP Energies nouvelles*, 68, 165–178, (2013).
- [26] Jiang Y., Yu Y., Huang J., Cai W., Marco J., “Li-ion battery temperature estimation based on recurrent neural networks”, *Science China Technological Sciences*, 64(6): 1335-1344, (2021).
- [27] Chen, L., Hu, M., Cao, K., Li, S., Su, Z., Jin, G., Fu, C., “Core temperature estimation based on electro-thermal model of lithium-ion batteries”, *International Journal of Energy Research*, 44, 5320–5333, (2020).
- [28] Pang, H., Guo, L., Wu, L., Jin, J., Zhang, F., Liu, K., “A novel extended Kalman filter-based battery internal and surface temperature estimation based on an improved electro-thermal model”, *The Journal of Energy Storage*. 41. 102854, (2021).
- [29] Torchio, M., Magni, L., Gopaluni, R. B., Braatz, R. D., Raimondo, D. M., “Lionsimba: a matlab framework based on a finite volume model suitable for li-ion battery design, simulation, and control,” *Journal of The Electrochemical Society*, 163, 7, A1192, (2016).
- [30] Saqli K., Bouchareb H., M’Sirdi N. K., Aziz N., Oudghiri M., “Electric and Thermal Model of Li-ion battery pack with cylindrical components”. *REDEC’20 the International Conference on Renewable Energy for Developing Countries*, Marrakech, Morocco, (2020).
- [31] Zhou W., Zheng Y., Pan Z., Lu Q., “Review on the Battery Model and SOC Estimation Method”, *Processes*, 9: 1685, (2021).
- [32] Thomas, K. E., Newman, J., “Thermal Modeling of Porous Insertion Electrodes”. *Journal of The Electrochemical Society*, 150, 2: A176, (2003).
- [33] Bernardi, D., Newman J., Pawlikowski E., “A General Energy Balance for Battery Systems”, *Journal of The Electrochemical Society*, 132(1): 5, (1985)